International Journal of Power Electronics and Drive System (IJPEDS)
Vol. 6, No. 1, March 2015, pp. 92~99
ISSN: 2088-8694

Comparison of Estimated Torques Using Low Pass Filter and Extended Kalman Filter for Induction Motor Drives

Ibrahim Mohd Alsofyani*, Nik Rumzi Nik Idris*, Yahya A. Alamri*, Tole Sutikno, Aree Wangsupphaphol*, Norjulia M. Nordin***
* UTM-PROTON Future Drive Laboratory, Power Electronics and Drives Research Group Faculty of Electrical Engineering, Universiti Teknologi Malaysia, 81310 Skudai, Johor, Malaysia
** Departement of Electrical Engineering, Universitas Ahmad Dahlan, Yogyakarta, Indonesia

Article Info

Article history:

Received Dec 12, 2014
Revised Jan 28, 2015
Accepted Feb 8, 2015

Keyword:

Estimated torques
Extended Kalman filter
Induction motor
Low pass filter
Real time control
Voltage/Hz control

ABSTRACT

Torque calculation process is one of the major concerns for controlling induction motors in industry, which requires very accurate state estimation of unmeasurable variables of nonlinear models. This can be solved if the variables used for torque calculation is accurately estimated. This paper presents a torque calculation based on a voltage model represented with a low-pass filter (LPF), and an extended Kalman filter (EKF). The experimental results showed that the estimated torque at low speed based on EKF is more accurate in the expense of more complicated and larger computational time.

Corresponding Author:

Ibrahim M. Alsofyani,
UTM-PROTON Future Drive Laboratory,
Power Electronics and Drives Research Group Faculty of Electrical Engineering,
Universiti Teknologi Malaysia,
81310 Skudai, Johor, Malaysia
Email: alsofyani2002@yahoo.com

1. INTRODUCTION

In the high-performance drives; field-oriented or direct torque control, accurate torque estimation is essential to avoid improper drive operation and to achieve a highly stable system. Most of the torque estimation techniques proposed so far are based on the voltage model (VM), or the current model (CM).

The voltage model is the common name for a stator flux estimator used in sensorless induction motor drives since the rotor speed information is not required for the stator flux estimation, and the only essential parameter of the model is the stator resistance [1]. The VM is normally used in a high speed range, since at low speed, some problems arise. There are two well-known problems if a pure integrator is used: (1) drift and eventually saturation in the estimated flux due to the presence of the DC offset in the measured current [1]-[2], and (2) extreme sensitivity to stator resistance mismatch due to temperature increase, notably at low speed when the stator voltage is low [3]. To overcome (1), a low-pass filter (LPF) is normally used in place of a pure integrator. However, this method reduces the performance of the system drive because of the phase and magnitude errors due to the LPF, especially when frequencies are close to the cutoff frequency [4]. An attempt to solve this drawback, Karanayil et. al. [5] have proposed a small-time-constant cascaded LPFs to reduce the DC offset decay time. Comanescu and Longya [6] have addressed flux estimation based on a phase locked loop (PLL) programmable LPF showing an improvement in the magnitude and phase of the estimated flux.

The current-model estimation, on the other hand, is normally applied at low frequency, and requires information on d and q stator current and rotor speed (or position) [2], [7]. In practice, accurate speed measurement is important for robust and precise control of IMs. However, the use of an incremental encoder to get the speed or position of the rotor is unattractive since it reduces the robustness and reliability of the drive, and increases hardware complexity and cost [8]. Thus, speed estimation techniques based on terminal variables that can replace mechanical speed sensors, have received increasing attention in recent decades. It is well-known that even though the use of CM has managed to remove the sensitivity to the stator resistor variation at low speed, on the other hand, it introduced parameter-sensitivity due to the rotor parameter variations, especially at high speed region. To address this problem, various methods have been proposed. For instance, Salmasi and Najafabadi [9] have proposed an adaptive observer which is capable of concurrent estimation of stator currents and rotor fluxes with online adaptation of rotor and stator resistances. Toliyat *et al.* [10] have developed artificial neural networks (ANNs) in closed loop observer for estimating rotor resistance and mutual inductance. There is also a stochastic approach that uses extended Kalman filter (EKF) in estimating the variables of an induction motor (IM), such as speed, torque, and flux [3]. Using EKF-based observer, it is possible to estimate the unknown parameters of IM, taking into account the parameter variations and measurement noises, in a relatively short time interval [11]-[16].

This paper investigates the real time calculation of torque using the estimated state variables based on the LPF filter and EKF and then compares them with simulated torques. In this way, it will be shown which technique is closer to simulation. The paper is organized in five sections. The following section presents the EKF-based torque calculator. Section 3 deals with the low pass filter, which represents the voltage model. Simulation and experimental results are presented in Sections 4. Finally, section 5 concludes the work.

2. EXTENTDED KALMAN FILTER ALGORITHM

In this study, EKF is used to concurrently estimate current, rotor flux, and rotor speed for speed sensorless control of IMs. However, the precise estimation of these state variables is very much reliant on how well the filter matrices are selected over a wide speed range [17]. The extended model to be used in the development of the EKF algorithm can be written in the following general form (as referred to the stator stationary frame.

$$\dot{x}_i(t) = f_i(x_i(t), u(t)) + w_i(t) \tag{1}$$

$$f_i(x_i(t), u(t)) = A_i(x_i(t))x_i(t) + Bu(t) \tag{2}$$

$$Y(t) = H_i(x_i(t))x_i(t) + Bu(t) + v_i(t) \tag{3}$$

There i = 1, 2, extended state vector x_i is representing the estimated states, f_i is the nonlinear function of the states and inputs, A_i is the system matrix, u is the control-input vector, B is the input matrix, w_i is the process noise, H is the measurement matrix, and v_i is the measurement noise. The general form of IM can be represented by (4) and (5).

$$\underbrace{\begin{bmatrix} \dot{i}_{sd} \\ \dot{i}_{sq} \\ \dot{\psi}_{rd} \\ \dot{\psi}_{rq} \\ \dot{\omega}_r \end{bmatrix}}_{\dot{X}} = \underbrace{\begin{bmatrix} -\left(\frac{R_s}{L_\sigma} + \frac{L_m^2 R_r}{L_\sigma L_r^2}\right) & 0 & \frac{L_m R_r}{L_\sigma L_r^2} & \frac{\omega_r L_m}{L_\sigma L_r} & 0 \\ 0 & -\left(\frac{R_s}{L_\sigma} + \frac{L_m^2 R_r}{L_\sigma L_r^2}\right) & -\frac{\omega_r L_m}{L_\sigma L_r} & \frac{L_m R_r}{L_\sigma L_r^2} & 0 \\ \frac{R_r}{L_r} & 0 & -\frac{R_r}{L_r} & -\omega_r & 0 \\ 0 & \frac{R_r}{L_r} L_m & \omega_r & -\frac{R_r}{L_r} & 0 \\ 0 & 0 & 0 & 0 & 0 \end{bmatrix}}_{A} \underbrace{\begin{bmatrix} i_{sd} \\ i_{sq} \\ \psi_{rd} \\ \psi_{rq} \\ \omega_r \end{bmatrix}}_{X} + \underbrace{\begin{bmatrix} 1/L_\sigma & 0 \\ 0 & 1/L_\sigma \\ 0 & 0 \\ 0 & 0 \\ 0 & 0 \end{bmatrix}}_{B} \cdot \underbrace{\begin{bmatrix} v_{sd} \\ v_{sq} \end{bmatrix}}_{u} + w(t) \tag{4}$$

$$\begin{bmatrix} i_{sd} \\ i_{sq} \end{bmatrix} = \underbrace{\begin{bmatrix} 1 & 0 & 0 & 0 & 0 \\ 0 & 1 & 0 & 0 & 0 \end{bmatrix}}_{H} \cdot \underbrace{\begin{bmatrix} i_{sd} \\ i_{sq} \\ \psi_{rd} \\ \psi_{rq} \\ \omega_r \end{bmatrix}}_{X} + v(t) \tag{5}$$

Where i_{sd} and i_{sq} are the d and q components of stator current, Ψ_{rd} and Ψ_{rq} are d-q rotor flux components, ω_r is the rotor electric angular speed in rad/s, v_{sd} and v_{sq} are the stator voltage components, L_s, $L_r$and L_m are the stator, rotor and mutual inductances respectively, R_s is the stator resistance, and R_r is the rotor resistance.

In this section, the EKF algorithm used in the IM model will be derived using the extended model in (4) and (5). For nonlinear problems, such as the one in consideration, the KF method is not strictly applicable, since linearity plays an important role in its derivation and performance as an optimal filter. The EKF technique attempts to overcome this difficulty by using a linearized approximation, where the linearization is performed about the current state estimate. This process requires the discretization of (4) and (5) as follows:

$$\dot{x}_i(k+1) = f_i(x_i(k), u(k)) + w_i(k) \tag{6}$$

$$f_i(x_i(k), u(k)) = A_i(x_i(k))x_i(k) + Bu(k) \tag{7}$$

$$Y(k) = H_i(x_i(k))x_i(k) + Bu(k) + v_i(k) \tag{8}$$

The linearization of (7) is performed around the current estimated state vector $\hat{x}_i$ given as follows.

$$F_i(k) = \left. \frac{\partial f_i(x_i(k), u(k)}{\partial x_i(k)} \right|_{\hat{x}_i(k)} \tag{9}$$

The resulting EKF algorithm can be presented with the following recursive relations:

$$P(k) = F(k)P(k)F(k)^{-1} + Q \tag{10}$$

$$K(k+1) = H^T P(k)(HP(k+1)H^T + R)^{-1} \tag{11}$$

$$\hat{x}(k+1) = \hat{f}(x(k), u(k)) + K(k)(Y(k) - H\hat{x}(k)) \tag{12}$$

$$P(k+1) = (I - K(k+1)H)P(k) \tag{13}$$

In (10)-(13)Q is the covariance matrix of the system noise, namely, model error, R is the covariance matrix of the output noise, namely, measurement noise, and P are the covariance matrix of state estimation error. The algorithm involves two main stages: prediction and filtering. In the prediction stage, the next predicted states $\hat{f}(\cdot)$ and predicted state-error covariance matrices, $\hat{P}(\cdot)$ are processed, while in the filtering stage, the next estimated states $\hat{x}(k+1)$ obtained as the sum of the next predicted states and the correction term [second term in (12)], are calculated. The structure of the EKF algorithm is shown in Figure 1.

The electromagnetic torque based on EKF is expressed based on the selected state variables which are the stator current and rotor fluxr:

$$T_e = \frac{3}{2}\frac{p}{2}\frac{L_m}{L_r}\left(i_{sq}\psi_{dr} - i_{sd}\psi_{qr}\right) \tag{14}$$

The electromagnetic torque based on EKF is expressed based on the selected state variables which are the stator current and rotor flux.

3. VOLTAGE-MODEL-BASED TORQUE ESTIMATOR

The stator flux estimation based on the voltage model is derived from the stator voltage equation given by:

$$\bar{v}_s = R_s i_s + \frac{d\bar{\psi}_s}{dt}.$$

The stator flux, therefore, can be written as:

$$\bar{\psi}_s = \int (\bar{v}_s - \bar{i}_s R_s) dt. \tag{15}$$

Under sinusoidal steady-state condition, this reduces to:

$$j\omega_e \bar{\psi}_S = \bar{v}_S - \bar{i}_S R_S.$$

$$\bar{\psi}_s = \frac{\bar{v}_s - \bar{i}_s R_s}{j\omega_e}. \tag{16}$$

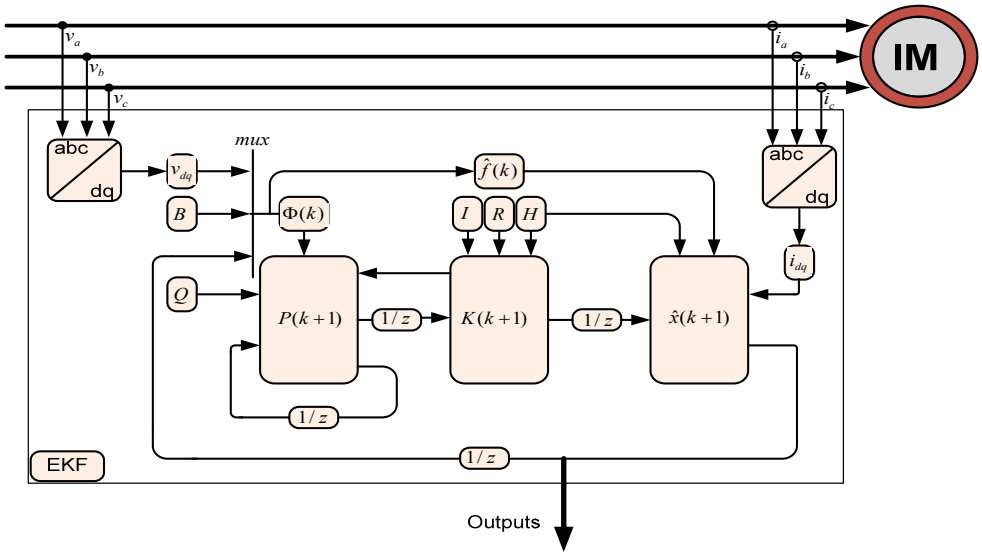

Figure 1. Structure of extended Kalman filter

To avoid the integration drift problem due to the dc offset or measurement noise, an LP filter is normally used in place of the pure integrator. With an LP filter, (16) becomes

$$\bar{\psi}'_s = \frac{\bar{v}_s - \bar{i}_s R_s}{j\omega_e + \omega_c}. \tag{17}$$

where ω_c is the cutoff frequency of the LP filter in radians per second and $\bar{\psi}'_s$ is the estimated stator flux which is obviously not equal to ψ_s of (16).

Choosing a cutoff frequency which is closer to the operating frequency will reduce the dc offset in the estimated stator flux, which on the other hand will introduce phase and magnitude errors.

The electromagnetic torque equation for LPF is calculated based on the estimated stator flux and measured stator current:

$$T_e = \frac{3}{2}\frac{p}{2}\left(\bar{\psi}'_{sd} i_{sq} - \bar{\psi}'_{sq} i_{sd}\right) \tag{18}$$

4. SIMULATION AND EXPERIMENTAL RESULTS

In order to study the performance and feasibility of the estimators, experimental results obtained from both the EKF- and LPF-based estimators are compared with the results obtained from simulations using Matlab/SIMULINK. In both simulations and experiments, the induction motor is run using constant Volts per Hertz (V/Hz) control scheme. In the experiment, the torque is calculated using the LPF and EKF-based estimators. The calculated torque from the experiment is then compared with the ideal or 'actual' torque directly obtained from the induction motor SIMULINK block in the simulation. The parameters of the induction motor used in the simulation and experiment are as shown in Table 1.

The experimental set-up consists of an insulated-gate bipolar transistor inverter, a dSPACE 1104 controller card, XILINX field programmable gate array (FPGA) and a 1.5-kW 4-pole squirrel-cage induction motor. An incremental encoder with 1024 ppr is used to measure the rotor speed.For safety reason, the DC voltage is limited to 100 V, which means that the based speed is reduced to 28 rad/s. The main tasks of the dSPACE are to produce the PWM control signals using the constant V/Hz scheme and, more importantly, to estimate the torque using LPF and EKF algorithms. The FPGA device is used for blanking time generation. The sampling period of the constant V/Hz scheme, including the state estimators, is 280 µs.

The initial values of the *P, R* and *Q* in the EKF algorithm are found by trial-and-error to achieve a rapid initial convergence as well as the desired transient- and steady-state performance. Thus, the initial values for EKF scheme – $P= diag[1\ 1\ 1\ 1\ 1]$, $Q = diag[10^{-10}\ 10^{-10}\ 10^{-12}\ 10^{-12}\ 10^{-3}]$, $R=diag[10^{-2}\ 10^{-2}\ ]$. As for LPF, the estimated stator flux is based on the cutoff frequency set to 5 rad/s.

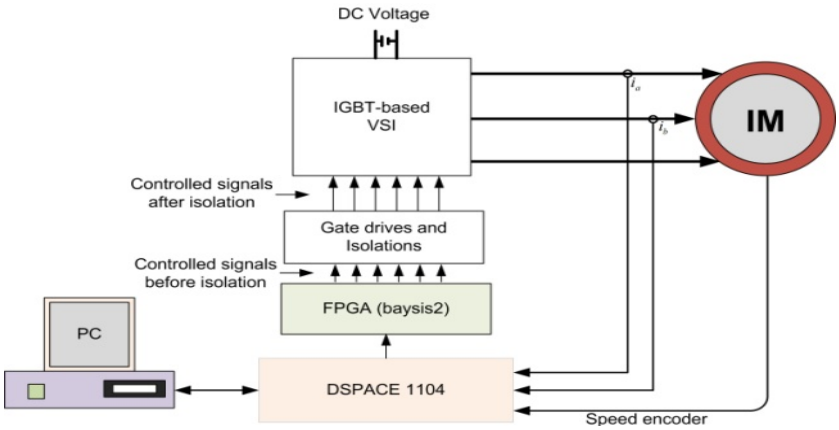

Figure 2. Schematic representation of the experimental setup

Table 1. Induction Motor Parameters

R_s [Ω]	R_r [Ω]	L_s [H]	L_r [H]	L_m [H]	J_L [Kg. m^2]	F
3	4.1	0.3419	0.3513	0.324	0.00952	4

The constant V/Hz drive, both in simulation and experiment, is run in an open loop mode where a step change in the speed reference from 0 to 28 rad/s is applied at t=2.8s.

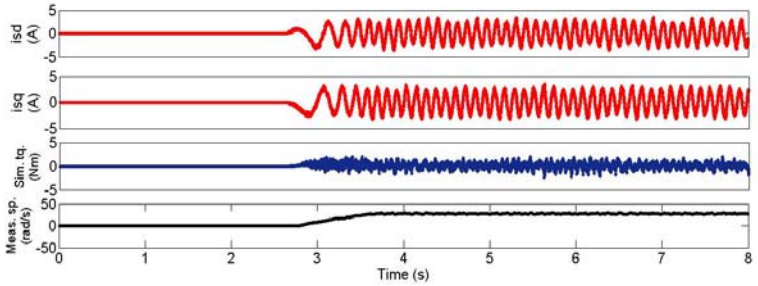

Figure 3. Simulation results: d-q stator current, torque, and speed

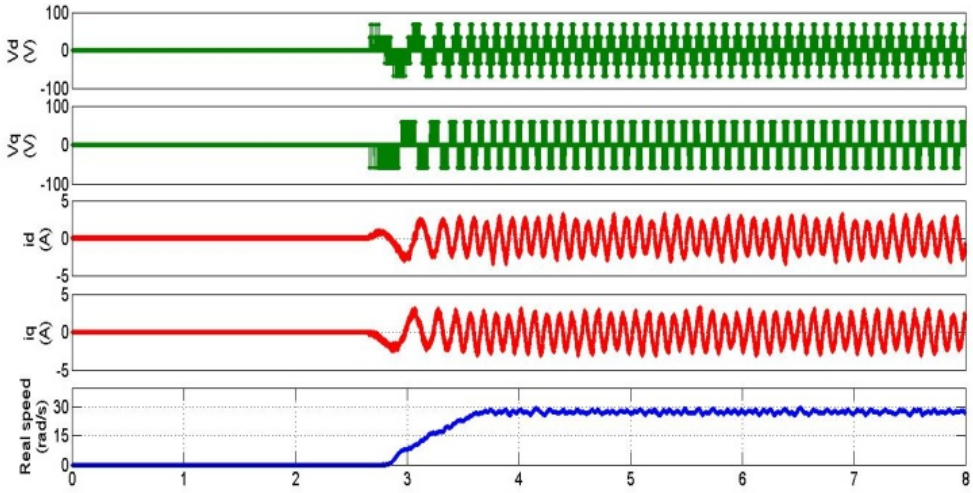

Figure 4. Experimental results: d-q stator voltage, d-q stator current, and measured speed

Figure 3 shows the simulation results, under ideal condition, of the d-q stator currents, simulated torque and rotor speed. Figure 4 shows the results obtained from experiment for the measured d-q stator currents and voltages, and speed, under the same condition. The performance of the EKF algorithm is evaluated experimentally through the estimated speed and the calculated torques as shown in Figure 5. In order to further examine the differences between the simulated and calculated torque based on EKF estimator, the waveforms are zoomed and shown Figure 8(a), where the differences (error) are also plotted. The EKF not only can be used to estimate the torque, but also can be utilized to estimate the speed; the estimated speed and measured speed obtained from experiment is shown in Figure 6. It can be seen that estimated and measured speeds almost coincided except at start-up, where significant error can be observed due to the lack of flux rotation at zero speed.

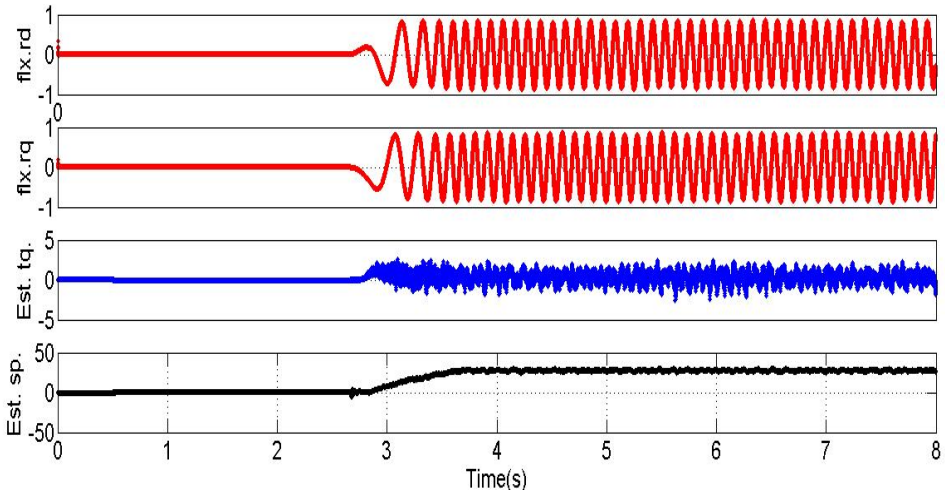

Figure 5. Experimental results: d-q rotor flux, estimated torque, and estimated speed for EKF

The experimental results of the d-q axes of the estimated stator flux, and the magnitude of the calculated torque with the LPF cutoff frequency set to 5 rad/s is shown in Figure 7. The differences between the calculated torque based on LPF voltage model and the simulated torque can be clearly seen in Figure 8(b), where the waveforms are zoomed. Examining Figure 8(a) and 8(b), one can clearly see the torque estimation using LPF is poor because of the uncertainties of parameters, nonlinearty of the inverters, measurement noise of current. For these reasons, the EKF observer is used as it can take into account all of these uncertainties and noises. This can be proved by inspected the narrower error band of the EKF torque.

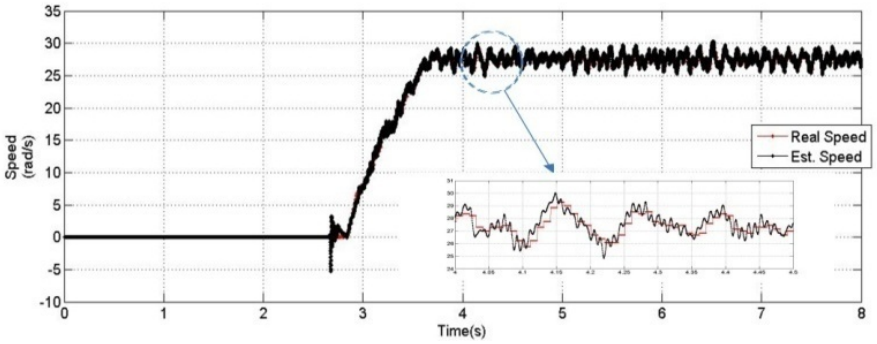

Figure 6. Experimental results: Measured and estimated speed obtained from EKF estimator

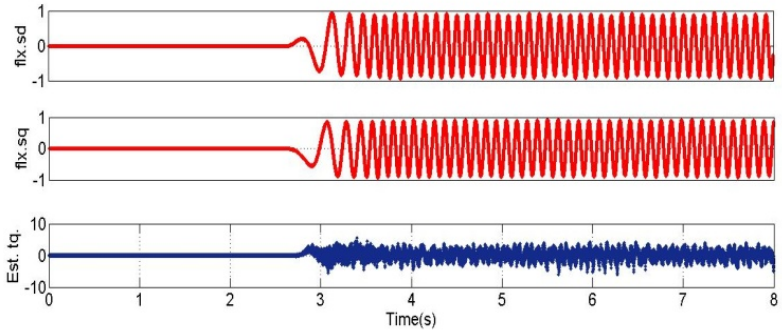

Figure 7. Experimental results: d-q stator flux and estimated torque based on voltage model (LPF)

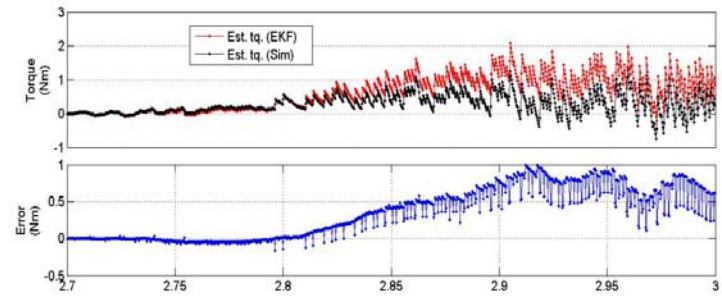

(a)

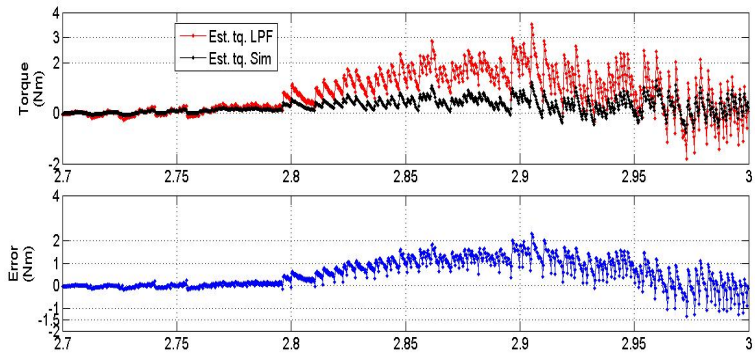

(b)

Figure 8. Comparison between the torques obtained from the simulation and experiment for (a) EKF, (b) LPF

4. CONCLUSION

In this paper, a comparison of state estimations for torque calculation based on EKF and LPF filters applied for an induction motor control has been performed. The performances of the EKF and LPF schemes under the same conditions are experimentally evaluated by comparing them with the results obtained from the simulation. When comparing both results, the EKF-based state estimation shows much better accuracy than the LPF-based state estimation in calculating the torque. The EKF-based is also capable of estimating the speed under transient and steady state conditions. The drawback of EKF-based estimation is the large sampling time due to the complex mathematical equations involved.

REFERENCES

[1] JW Finch, D Giaouris, Controlled AC Electrical Drives, *IEEE Trans. Ind. Electron,* 2008; 55: 481-491.
[2] IM Alsofyani, NRN Idris, A review on sensorless techniques for sustainable reliablity and efficient variable frequency drives of induction motors, *Renewable and Sustainable Energy Reviews,* 2013; 24: 111-121.
[3] IM Alsofyani*, et al.*, Evaluation of Speed and Torque Estimations for the EKF-based Direct Torque Control in Induction Machines, *TELKOMNIKA Indonesian Journal of Electrical Engineering,* 2014; 12: 7659-7667.
[4] NRN Idris, AHM Yatim, An improved stator flux estimation in steady-state operation for direct torque control of induction machines, *IEEE Trans. Ind. Appl.,* 2002; 38: 110-116.
[5] B Karanayil*, et al.*, An implementation of a programmable cascaded low-pass filter for a rotor flux synthesizer for an induction motor drive, *IEEE Trans. Power Electron.,* 2004; 19: 257-263.
[6] M Comanescu, X Longya, An improved flux observer based on PLL frequency estimator for sensorless vector control of induction motors, *IEEE Trans. Ind. Electron.,* 2006; 53: 50-56.
[7] J Holtz, Sensorless Control of Induction Machines;With or Without Signal Injection?, *IEEE Trans. Ind. Electron,* 2006; 53: 7-30.
[8] M Barut*, et al.*, Experimental Evaluation of Braided EKF for Sensorless Control of Induction Motors, *IEEE Trans. Ind. Electron,* 2008; 55: 620-632.
[9] FR Salmasi, TA Najafabadi, An Adaptive Observer With Online Rotor and Stator Resistance Estimation for Induction Motors With One Phase Current Sensor, *IEEE Trans. Energy Convers,* 2011; 26: 959-966.
[10] HA Toliyat*, et al.*, Neural-Network-Based Parameter Estimations of Induction Motors, *IEEE Trans. Ind. Appl.,* 2008; 55: 1783-1794.
[11] IM Alsofyani*, et al.*, *Improved EKF-based direct torque control at the start-up using constant switching frequency*, Energy Conversion (CENCON), 2014 IEEE Conference, 2014; 237-242.
[12] IM Alsofyani, NRN Idris, I*mproved sensorless EKF-based direct torque control at low speed with constant switching frequency controller*, Power Engineering Conference (AUPEC), Australasian Universities, 2014; 1-5.
[13] IM Alsofyani*, et al.*, *An optimized Extended Kalman Filter for speed sensorless direct troque control of an induction motor*, Proc. Int. Power and Energy, 2012; 319-324.
[14] IM Alsofyani*, et al.*, *Using NSGA II multiobjective genetic algorithm for EKF-based estimation of speed and electrical torque in AC induction machines*, Proc. Int. Power Engineering and Optimization, 2014; 396-401.
[15] Hisham Alrawashdeh, JA Sumadu, The Kalman Filter Performance for Dynamic Change in System Parameters, *International Journal of Electrical and Computer Engineering,* 2013; 3(6): 713-723.
[16] L Liu, Improved Reaching Law Sliding Mode Control Algorithm Design for DC Motor Based on Kalman Filter, *TELKOMNIKA Indonesian Journal of Electrical Engineering,* 2014; 12(12): 8193-8199.
[17] S Buyamin, JW Finch, *Comparative Study on Optimising the EKF for Speed Estimation of an Induction Motor using Simulated Annealing and Genetic Algorithm*, IEEE Proc. IEMDC Conf., 2007; 1689-1694.